ChemComm

Accepted Manuscript

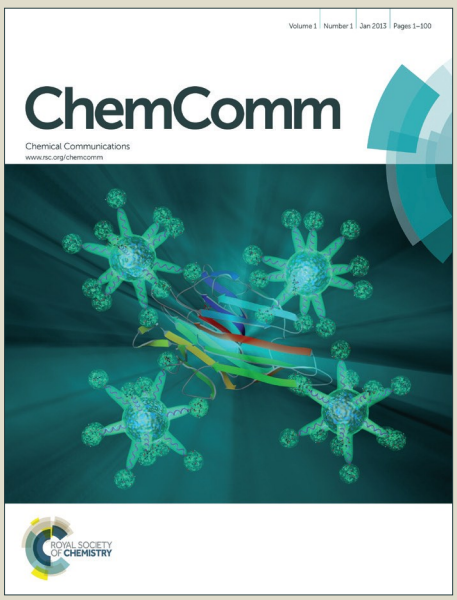

ROYAL SOCIETY OF CHEMISTRY

www.rsc.org/chemcomm

ChemComm

RSCPublishing

ARTICLE

Optimization of Gold Nanoparticle Photoluminescence by Alkanethiolation

Cite this: DOI: 10.1039/xoxxoooooox

Sheng-Feng Lai,[a,b] Hui-Ru Tan,[c] Eng-Soon Tok,*[d] Yu-Han Chen,[b] Edwin B. L. Ong,[b] Min-Tsang Li,[b] Yi-Yun Chen,[b] Fan-Ching Chien,[e] Peilin Chen,[f] G. Margaritondo[g] and Y. Hwu*[a,b,h]

Received ooth January 2012,
Accepted ooth January 2012

DOI: 10.1039/xoxxoooooox

www.rsc.org/

Surface thiolation affects the size of gold nanoparticles and the presence of visible luminescence under UV stimulation. We explored these phenomena by analysing alkanethiolate coatings with different carbon chain lengths, from 3-mercaptopropionic acid to 16-mercaptohexadecanoic acid, synthesized by intense x-ray irradiation. Photoluminescence is present for the smallest nanoparticles, but its intensity becomes more intense as the carbon chain length increases, achieving a 28% quantum efficiency with 16-mercaptohexadecanoic acid coating.

We recently discovered two important effects of 11-MUA (mercaptoundecanoic acid) coatings on gold nanoparticle (AuNPs). First, MUA coating under x-ray irradiation impedes the growth of nanoparticles beyond a very small (1 nm) size.[1] Second, a MUA-coated AuNPs luminesce with a very large Stokes shift in the visible when subject to UV light.[2,3] Motivated by their potential importance for applications, we expanded our analysis of such phenomena by studying a series of coatings in the same family (n-alkanethiolates): 3-MPA (3-mercaptopropionic acid), 6-MHA (6-mercaptohexanoic acid), 8-MOA (8-mercaptooctanoic acid) and 16-MHDA (16-mercaptohexadecanoic acid), all produced under x-ray irradiation. The main result is that the smallest nanoparticles are systematically photoluminescent, but for a given set of conditions the emission becomes more intense as the chain length increases. Furthermore, we found that the nanoparticle size can be tuned, for small surfactant-to-metal ratios in the solution, by selecting a coating with appropriate carbon chain length.

Besides their obvious fundamental interest, these findings could be exploited for applications.[4-10] The intense photoluminescence can be used to track AuNPs in biology specimens, for example to study fluid flows or the evolution of tumours and of the related microvasculature. And the AuNP size control is a general problem on the way of practical utilizations. Our approach could be an alternative to the accurate tuning of reaction processes and parameters, or to external confinements such as the use of templates.[11-15] Indeed, our coatings produced uniform particle sizes and clean nanoparticle surfaces, free of surfactants and reducing agents. This last characteristic is a result of the extremely rapid and uniform reduction.

The strategy of our study was directly suggested by the first results on 11-MUA coating. We speculated that the carbon chain length affected dipole structures on the surface and, through them, the photoluminescence. In other words, by changing the n-alkanethiolate coating compound, we could change the physical properties including luminescence while not significantly modifying the surface chemistry. We decided to empirically explore this possibility and found indeed a clear link between chain length and photoluminescence intensity.

The experiments were performed with reagent grade chemicals: $HAuCl_4 \cdot 3H_2O$, n-alkanethiolates and sodium hydroxide were purchased from Sigma-Aldrich. 0.5 mL of 20 mM $HAuCl_4 \cdot 3H_2O$ were adjusted to pH ~11 with 0.1 M NaOH. Afterward, we added the thiolates dissolved in anhydrous ethanol with specific thiolate-to-Au ratio (*R*) and DI water to reach a 10 mL volume. The solution was placed in polypropylene conical tubes and irradiated while stirring for 60 sec by using hard X-rays from the BL01A beamline of the NSRRC (Taiwan National Synchrotron Radiation Research Center), running at a constant electron current of 300 mA. The X-ray photon energy ranged from 8-15 keV and was centred at ~12 keV delivering a dose rate ~4.7×10^5 Gy s^{-1}.[16] After the irradiation, the solution was dialyzed against periodically changed DI water to remove ethanol and unbound thiolates.

UV-visible spectra were acquired over 200-800 nm using a USB4000 Fiber Optic spectrometer from Ocean Optics (Dunedin, USA) with a 1 cm path length quartz cuvette (Hellma®, Germany), and Photoluminescence spectra were measured at room temperature with a Cary Eclipse spectrophotometer (Varian, USA). Samples for TEM (transmission electron microscopy) and HAADF-STEM (high-angle annular dark field-scanning transmission electron microscopy) were prepared by scooping solution with an ultrathin carbon-coated copper grid held with tweezers and left to dry on a filter paper. STEM observations were performed in a FEI Titan 80-300kV S/TEM system operated with an accelerating voltage of 200 kV. For FTIR measurements, the spectra of dried samples on a silicon wafer were recorded in the spectral range 4000-1000 cm^{-1} using a Perkin-Elmer Spectrum One instrument.

The size and distribution of the thiolate-coated were characterized by small-angle X-ray scattering (SAXS) using Beamline 23A of NSRRC. All of the SAXS data were obtained using an area detector covering a *q* range from 0.01 to 0.1 $Å^{-1}$, and the incident angle of the X-ray beam (0.5 mm diameter) was fixed at 0.2° with an X-ray energy of 10 keV. Afterward, the size and distribution were analysed using the sphere-model fitting and the Guinier's law.[17,18]

For imaging characterization, the 11-MUA- and 16-MHDA-coated AuNP solutions were dropped, dried at room temperature on microscope glass slides for multi-photon microscopy. The multi-photon microscope is equipped with a 25X water lens and a tuneable pulse laser (740-1260 nm wavelength).

Figure 1 shows UV-visible spectra of the Au NPs prepared in the presence of three different n-alkanethiolates: 3-MPA (3-mercaptopropionic acid), 6-MHA (6-mercaptohexanoic acid) and 8-MOA (8-mercaptooctanoic acid). The AuNPs were obtained with different R-values (R = the ratio of n-alkanethiolate concentration to metal ion concentration). The behaviour of the surface plasmon resonance (SPR) peak is consistent with the previous results on 11-MUA: the AuNP size progressively decreases as the R-value increases.

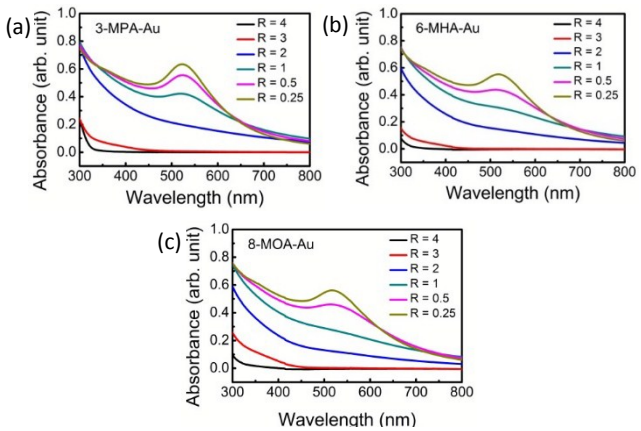

Fig. 1 UV-visible spectra of colloidal Au NCs synthesized in the present of the (a) 3-MPA, (b) 6-MOA, and (c) 8-MUA with different R-values.

The TEM images in Fig. 2 show that the decreasing size of the AuNPs coated with 3-MPA, 6-MHA, 8-MOA, 11-MUA and 16-MHDA at R = 0.25: 8.38±2.28, 6.65±1.39, 5.85±1.36, 5.35±1.09 and 5.24±1.26 nm. This can be explained noting that shorter carbon-chain n-alkanethiolates have lower reactive binding probability to gold since the decreasing carbon chain length increases the activation barrier for the S-H bond dissociation.[19]

Figure 3 shows HAADF-STEM images of thiolate-coated AuNPs for R = 3. The average size is ~1.3 nm for all n-alkanethiolates. The link between AuNP size and carbon-chain length is further illustrated in Fig. 4. The main messages are that the chain length influences the nanoparticle size, but that this is true only for small R-values. This is not unexpected, since for large R-values all n-alkanethiolates result in a very fast coating.

Figure 5 (a) shows the results SAXS for AuNPs with different n-alkanethiolates coatings at R = 3. Such results are presented as ln(I) vs q^2 , where I is the scattered intensity and q is the scattering vector, and were extracted from raw SAXS patterns (Fig. S1). From SAXS data, we extracted the nanoparticle sizes shown in Fig. 5 (b), revealing a marked increase as the carbon chain length increases. Dynamic light scattering (DLS) measurements (Fig. S5) show the same trend of increasing overall particles size as that of SAX measurements.

How can this be reconciled with the constant size given by HAADF-STEM (Figs. 3 and 4)? Quite simply, the sizes measured by SAXS and DLS correspond to the entire nanosystem, metal core plus coating, whereas HAADF-STEM only detects the core. Thus, the growing nanoparticle size revealed by SAXS is due to the increasing thickness of the coating as the chain length increases. Such conclusion is confirmed by FTIR analysis (Fig. S2) showing that the coating methylene bands at 2,920 and 2,848 cm^{-1} become more intense as the chain length increases; this also demonstrates the integrity of the chain length during x-ray irradiation.

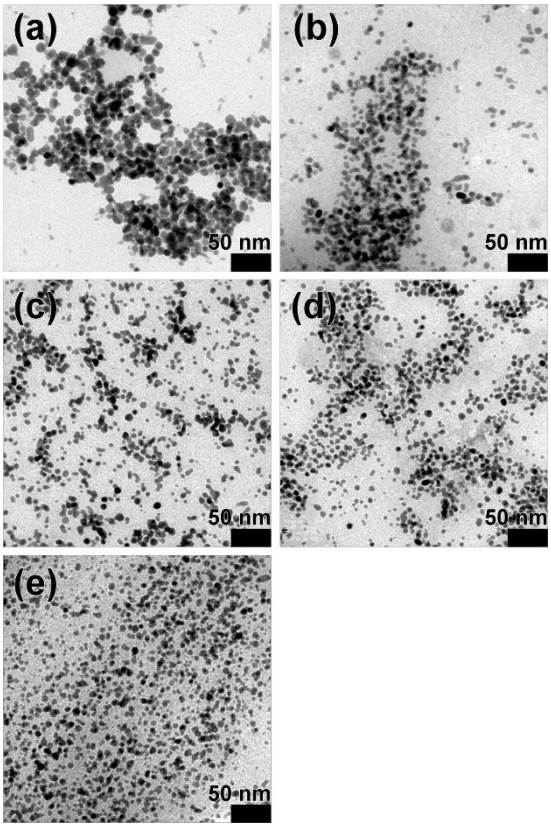

Fig. 2 TEM micrographs of the thiolate-coated Au NPs with R = 0.25. (a) 3-MPA-Au NPs; (b) 6-MHA-Au NPs; (c) 8-MOA-Au NPs; (d) 11-MUA-Au NPs; (e) 16-MHDA-Au NPs. Bars: 50 nm.

We now turn again our attention to photoluminescence. Figure 6 illustrates the effect of the carbon chain length on the photoluminescence intensity (excited by 240 nm wavelength UV radiation) and absorbance of AuNPs. For carbon numbers below eight, photoluminescence is detected but rather weak; then, its intensity increases with the carbon number (Fig. 6 (a)). Since the peak position has been reported to change with the particle size,[20,21] our observation of a fixed emission peak position at 618 nm is consistent with our HAADF-STEM result that reveal the same core size for all coatings. Note that, whereas the peak wavelength is independent of the coating, the peak intensity does increase with the carbon number of the alkanethiolates.

Figure 6 (b) shows an absorption peak at 240 nm, particularly prominent for the longer chain n-alkanethiolates. The analysis of photoluminescence indicates that the optimal excitation wavelength is also 240 nm (Fig. S3).

From absorption and photoluminescence results we calculated the quantum yield (QY, Φ_i) by using a standard phenylalanine (QY: 2.2% in water) and the following equation:[22]

$$\Phi_i = \frac{F_i f_s}{F_s f_i}\Phi_s$$

where F_i and F_s are the integrated emission areas of the standard and sample spectra; f_i and f_s are the absorption factors for the standard and samples that calculated by $f = 1\text{-}10^{-A}$ (where A is the absorbance at 240 nm wavelength). The results of Figure S4 show that we were within the linear range of the emission-to-absorption curves, ruling out self-quenching effect.

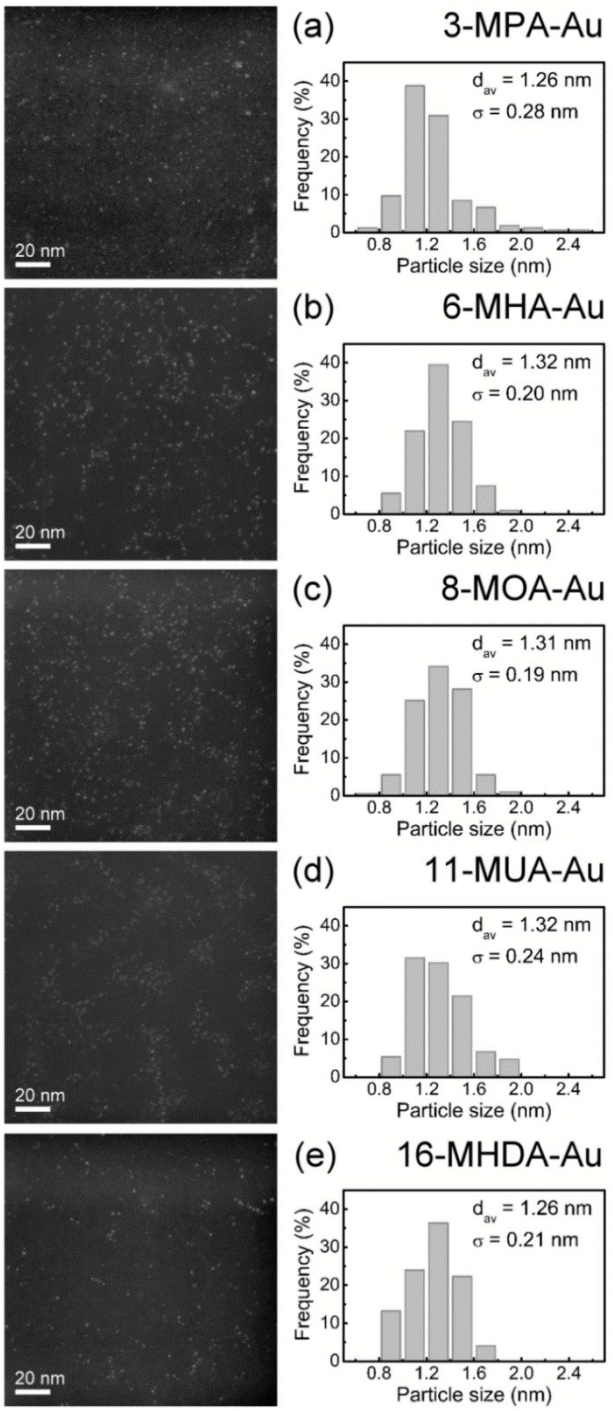

Fig. 3 HAADF-STEM micrographs of AuNPs synthesized in the presence of (a) 3-MPA, (b) 6-MHA, (c) 8-MOA, (d) 11-MUA, and (e) 16-MHDA with R = 3. The right side shows the corresponding size histograms (n>200).

Figure 7 (a) shows the increase of quantum yield as the carbon number increases. Very high quantum ratio, ~28%, is achieved by the 16 MHDA-AuNPs. Thus, the chain length is beneficial not only for the photoluminescence intensity but also for its efficiency. The total performance of fluorophores is normally gauged by another parameter: the molar extinction coefficient (EC) which is defined as the absorbance/path length of photon/sample concentration. The total emission is therefore a product of EC and QR. Figure 7 (b) shows the results of our measurement of EC of the AuNP with different thiolates which indicated that coating with molecules of longer carbon chain length also increases the photoluminescent performance.

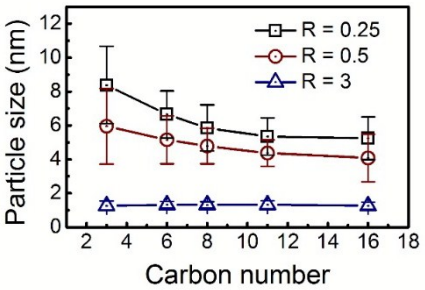

Fig. 4 The average size of the Au NPs plotted vs. the carbon number of the coating thiolate for R = 0.25, 0.5 and 3.

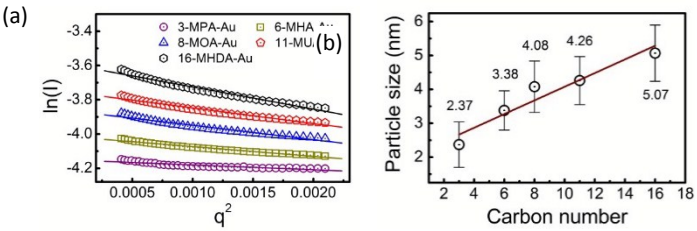

Fig. 5 (a) Plot of ln(I) vs q^2 for SAXS analysis; (b) Plot of entire particle size vs. the carbon number of thiolate coating.

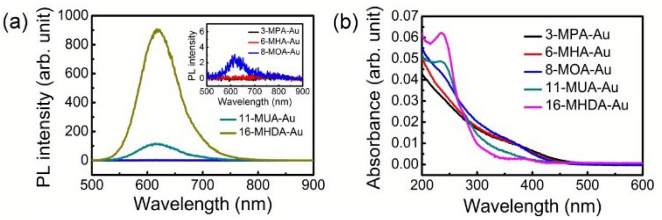

Fig. 6 (a) Photoluminescence and (b) UV-visible spectra of the AuNPs coated with different types of the thiolates: 3-MPA, 6-MHA, 8-MOA, 11-MUA, and 16-MHDA. The R-value and Au concentration are 3 and 4 μM.

Note that all the thiolates on the surface of AuNPs can be used as a convenient linker for bind the AuNPs with other organic molecules and acts as labeling fluorophores. Without making such a surface conjugation, we tested these photoluminescent AuNPs for fluorescent confocal microscopy applications. Figure 8 shows the result of these preliminary tests using a multi-photon excitation laser confocal microscopy. The 16-MHDA coated AuNPs indeed show strong photoluminescence after being internalized by the HeLa cells without other surface modifications. Conjugation of these AuNPs with antibodies to perform specific labeling and the characterization of the corresponding optical properties are underway. Preliminary results also show that the surface conjugation does not affect the photoluminescent properties of the AuNPs.

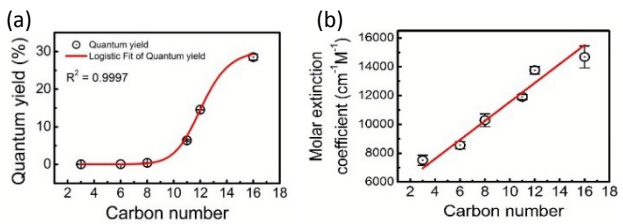

Fig. 7 (a) The quantum yield of the thiolate-coated AuNPs vs. the carbon number of the thiolates. (b) Molar extinction coefficient of the thiolate-coated AuNPs vs. the carbon number of the thiolates.

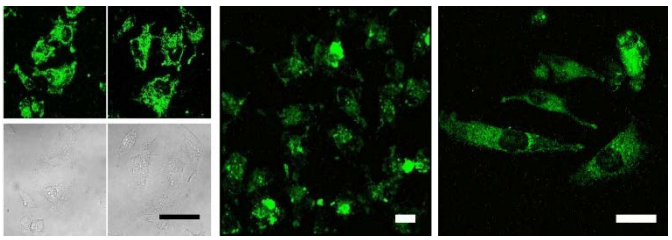

Fig. 8 (Left) Multi-photon excitation microscopy images (top row) and differential interference contrast (DIC) images (bottom row) of 16-MHDA-AuNP loaded HeLa cells. (Middle and Right) Larger area view of the multi-photon excitation microscopy image. The photoluminescent AuNPs are internalized in the cytoplasm. Bars: 50 μm.

What is the cause of the enhanced photoluminescence? This issue is no entirely clear. We could hypothesize two possible kinds of explanations. The first is a size effect affecting the local quantum states and the corresponding optical transitions. The second is a self-absorption effect: longer chain coatings cause less absorption, allowing the photoluminescence to reach vacuum. Based on the overall results and in particular the enhancement associated with the increase of carbon chain length of the alkanethiolates, we tend to favour the second explanation, but have no sufficient evidence to rule out the first, or other alternatives. The much longer photoluminescence lifetime, ~6.8 μs for 11-MUA coated AuNPs, as reported on Au nanoclusters at ns level, also indicates the photoluminescence of our AuNPs is most likely due to ligand-metal charge transfer.

Whatever is the cause, one must note the high levels of intensity and efficiency given by the longest chains: since practical applications were already possible with 11-MUA, there is promise of even more utilizations in the future. Furthermore, our AuNPs have very long shelf lives (several months), during which photoluminescence did not appreciably change (Fig. S7).

Acknowledgements

Work supported by Minister of Science and Technology, the Thematic Research Project of Academia Sinica, the National Synchrotron Radiation Research Center (Taiwan), the Fonds National Suisse pour la Recherche Scientifique and the Center for Biomedical Imaging (CIBM, supported by the Louis-Jeantet and Leenards foundations).

Notes and references

[a] Department of Engineering Science, National Cheng Kung University, Tainan 701, Taiwan
[b] Institute of Physics, Academia Sinica, Taipei 115, Taiwan
[c] Institute of Materials Research and Engineering, 3 Research Link, Singapore 117602
[d] Physics Department, National University of Singapore, Singapore 117542
[e] Department of Optics and Photonics, National Central University, Chun-Li 320, Taiwan
[f] Research Center for Applied Sciences, Academia Sinica, Taipei 115, Taiwan
[g] Ecole Polytechnique Fédérale de Lausanne (EPFL), CH-1015 Lausanne, Switzerland
[h] Advanced Optoelectronic Technology Center, National Cheng Kung University, Tainan 701, Taiwan

Electronic Supplementary Information (ESI) available: See DOI: 10.1039/b000000x/

1 S. F. Lai, W. C. Chen, C. L. Wang, H. H. Chen, S. T. Chen, C. C. Chien, Y. Y. Chen, W. T. Hung, X. Q. Cai, E. R. Li, I. M. Kempson, Y. Hwu, C. S. Yang, E. S. Tok, H. R. Tan, M. Lin and G. Margaritondo, *Langmuir*, 2011, **27**, 8424.
2 S. F. Lai, C. C. Chien, W. C. Chen, Y. Y. Chen, C. H. Wang, Y. Hwu, C. S. Yang and G. Margaritondo, *RSC Adv.*, 2012, **2**, 6185.
3 S. F. Lai, C. C. Chien, W. C. Chen, H. H. Chen, Y. Y. Chen, C. L. Wang, Y. Hwu, C. S. Yang, C. Y. Chen, K. S. Liang, C. Petibois, H. R. Tan, E. S. Tok and G. Margaritondo, *Biotechnol. Adv.*, 2013, **31**, 362.
4 H. Y. Chang, H. T. Chang, Y. L. Hung, T. M. Hsiung, Y. W. Lin and C. C. Huang, *RSC Adv.*, 2013, **3**, 4588.
5 T. G. Schaaff, G. Knight, M. N. Shafigullin, R. F. Borkman and R. L. Whetten, *J. Phys. Chem. B*, 1998, **102**, 10643.
6 J. P. Wilcoxon and P. Provencio, *J. Phys. Chem. B*, 2003, **107**, 12949.
7 R. L. Donkers, D. Lee and R. W. Murray, *Langmuir*, 2004, **20**, 1945.
8 Y. Shichibu, Y. Negishi, H. Tsunoyama, M. Kanehara, T. Teranishi and T. Tsukuda, *Small*, 2007, **3**, 835.
9 M. A. H. Muhammed, S. Ramesh, S. S. Sinha, S. K. Pal and T. Pradeep, *Nano Res.*, 2008, **1**, 333.
10 X. Yuan, Z. T. Luo, Q. B. Zhang, X. H. Zhang, Y. G. Zheng, J. Y. Lee and J. P. Xie, *ACS Nano*, 2011, 5, 8800.
11 S. W. Li, L. Burel, C. Aquino, A. Tuel, F. Morfin, J. L. Rousset and D. Farrusseng, *Chem. Commun.*, 2013, **49**, 8507.
12 N. R. Jana, L. Gearheart and C. J. Murphy, Langmuir, 2001, 17, 6782.
13 V. N. Kuzovkov and E. A. Kotomin, *Solid State Ionics*, 1997, **101**, 451.
14 H. Weller, *Angew. Chem. Int. Ed. Engl.*, 1993, **32**, 41.
15 M. J. Hostetler, J. E. Wingate, C. J. Zhong, J. E. Harris, R. W. Vachet, M. R. Clark, J. D. Londono, S. J. Green, J. J. Stokes, G. D. Wignall, G. L. Glish, M. D. Porter, N. D. Evans and R. W. Murray, *Langmuir*, 1998, **14**, 17.
16 C. J. Liu, C. H. Wang, C. L. Wang, Y. Hwu, C. Y. Lin and G. Margaritondo, *J. Synchrotron Radiat.*, 2009, **16**, 395.
17 A. Guinier and G. Fournet, *John Wiley & Sons*, New York, 1955.
18 R. J. Roe, *Oxford University Press*, New York, 2000.
19 J. C. Love, L. A. Estroff, J. K. Kriebel, R. G. Nuzzo and G. M. Whitesides, *Chem. Rev.*, 2005, **105**, 1103.
20 C. A. J. Lin, T. Y. Yang, C. H. Lee, S. H. Huang, R. A. Sperling, M. Zanella, J. K. Li, J. L. Shen, H. H. Wang, H. I. Yeh, W. J. Parak and W. H. Chang, *ACS Nano*, 2009, **3**, 395.
21 J. Zheng, C. Zhang and R. M. Dickson, *Phys. Rev. Lett.*, 2004, **93**, 077402.
22 A. M. Brouwer. *Pure Appl. Chem.*, 2011, **83**, 2213.
23 J. Zheng, C. Zhou, M. Yu and J. Liu, *Nanoscale*, 2012, **4**, 4073.

